Effect of nucleic acid stain Syto9 on nascent biofilm architecture of *Acinetobacter* sp. BD413

R. GrayMerod*, L. Hendrickx, L.N. Mueller***, J.B. Xavier**** and S. Wuertz***

*Department of Civil and Environmental Engineering, University of California, Davis, One Shields Avenue, Davis, CA 95616, USA (E-mail: *rtmerod@ucdavis.edu; swuertz@ucdavis.edu*)

**Laboratory for Radiobiology and Microbiology, Belgian Nuclear Research Centre, Boeretang 200, B-2400 Mol, Belgium (E-mail: *lhendric@sckcen.be*)

***Instituto de Tecnologia de Quimica e Biológica, Universidade Nova de Lisboa, 2781-901 Oeiras, Portugal (E-mail: *Lukas@itqb.unl.pt*)

****Kluyver Laboratory for Biotechnology, Delft University of Technology, Julianalaan 67, 2628 BC Delft, The Netherlands (E-mail: *J.Xavier@tnw.tudelft.nl*)

Abstract Flow cells were utilized to determine the effects of repetitive Syto9 staining on developing *Acinetobacter* sp. BD413 biofilm and to identify features describing reproducible biofilm architecture at 63 × magnification. Syto9 is a general nucleic acid stain employed to visualize the entire microbial population of the biofilm and a component in the LIVE/DEAD® BacLight™ Bacterial Viability kits. CLSM images were quantified with the biofilm analysis software PHLIP to calculate six commonly used biofilm architecture characteristics. The characteristics biovolume and mean thickness were most reproducible when biofilms were grown in separate flow cells under controlled conditions, while roughness, porosity, total spreading and surface area to biovolume ratio exhibited inherent variability. Biovolume was more variable in separate flow cells than in channels of the same flow cell. However, even biofilms grown in channels of the same flow cell did not generate reproducible architectures based on the six characteristics. Results suggest difficulties in differentiating the effect of changes due to treatment from the natural variability of architecture development at the cellular level. Despite this high variability, biofilms only stained once developed into thicker structures containing more biomass than biofilms stained multiple times, suggesting that repeated staining with Syto9 affects architecture development. The application of Syto9 to monitor developing biofilms is not recommended.

Keywords Acinetobacter; biofilm architecture; CLSM; flow cell; reproducibility

Water Science & Technology **Vol 52 No 7 pp 195–202** © IWA Publishing 2005

Introduction

Confocal laser scanning microscopy (CLSM) is the preferred tool to study nascent biofilms without affecting biofilm physical structure or architecture. Usually, microbial cells have to be labelled with fluorescent proteins or be naturally fluorescent to allow online visualization of developing biofilms (e.g. Cowan *et al.*, 2000; Heydorn *et al.*, 2000a). However, mixed or undefined biofilms cannot be viewed because not all cells are expected to fluoresce. For this reason biofilms grown in parallel flow cells are sacrificed at various time points under the assumption that comparable biofilm structures form in the separate channels. To overcome this limitation recent work has involved the application of the nucleic acid stain Syto9, a component in the LIVE/DEAD® BacLight™ Bacterial Viability kit, to observe growing biofilms in one flow channel over time without the need to terminate individual channels at each time point (Xavier *et al.*, 2001, 2004). The objectives of this study were to: (i) investigate the utility of SIX common measures to describe biofilm architecture in systems generally considered to render reproducible biofilms; and (ii) ascertain the validity of the assumption that certain nucleic acid stains have no effect on developing biofilm architecture. By applying CLSM coupled with quantitative image analysis we described the biofilm architecture of a monoculture

biofilm of *Acinetobacter* sp. BD413, a well-characterized bacterial strain capable of forming relatively homogenous biofilms (Hendrickx *et al.*, 2003), after repetitive staining with Syto9. The biofilm analysis software PHLIP was utilized to calculate the structural features roughness, mean thickness, spatial spreading, surface area to volume ratio, biovolume and porosity. Statistical analysis was employed to determine whether repeated Syto9 staining significantly affected biofilm architecture and if structural features were reproducible among flow cells and among channels of the same flow cell. This work extends previous research on the utility of parameters derived from time resolved two-dimensional biofilm images to account for microscale heterogeneity and morphological structures and to verify reproducibility of biofilm experiments (Heydorn *et al.*, 2000a, b; Yang *et al.*, 2000).

Methods

Experimental setup

Biofilms of *Acinetobacter* sp. BD413 were grown in a three-channel, stainless steel flow cell (channel size 40 mm long × 4 mm wide × 4 mm high) (Kuehn *et al.*, 1998, 2001). The flow cell was placed on the motorized stage of a Zeiss LSM 510 CLSM (Carl Zeiss, Jena, Germany). Glass microscope cover slips glued with silicone to the top and bottom sealed the flow channels and served as the substratum for biofilm attachment. The system consisted of an LB medium reservoir, the flow cell, a peristaltic pump (Ismatec SA, Zurich, Switzerland), and a waste reservoir, interconnected by Tygon® flexible tubing. The assembled flow cell, reservoirs, and tubing were autoclaved prior to each experiment.

All channels were inoculated with an equal volume of BD413 cells growing exponentially in LB medium. Inoculated cells were allowed to settle for 2 h prior to starting medium flow at 2.5 ml/h. Biofilms were grown for 3 days to an apparent steady state (Hendrickx *et al.*, 2003) and then stained after 3, 4 and/or 5 days of development to determine if repetitive Syto9 staining had an effect on developing architecture. On day 3, Channel 1 was stained by temporarily switching the inlet medium to an LB solution containing 5 μM Syto9 (Molecular Probes, Eugene, OR, USA). After 1.5 mL of the Syto9 solution had entered the system, the inlet medium was switched back to LB and flow restarted. Prior to scanning, the flow channel was rinsed for 1 h. On day 4, Channels 1 and 2 were stained and scanned using the same method. All three channels were stained and scanned on day 5. The repetitive staining procedure meant that by day 5 channel 1 had been stained a total of three times, channel 2 had been stained twice and channel 3 had been stained once. The experiment was performed three times. An additional flow cell experiment was run with four channels to determine if biofilm architecture was reproducible between channels of the same flow cell. Biofilms were stained once on day 5.

Automated image acquisition

Scanning of flow cell channels was accomplished with the MultiTime Series macro supplied by Zeiss as part of the image acquisition software. The macro operates the motorised focusing and stage movement controls and enables automated acquisition of images from predetermined locations in the channel. The images were obtained using a 63 ×/1.2 NA (C-Apochromat) water immersion objective lens. A series of horizontal xy optical sections (1,024 × 1,024 pixels) were automatically obtained from 21 fields each with a substratum area of 146.25 μm × 146.25 μm to cover a total area of approximately 4.5×10^5 μm^2. Image stacks were acquired with a Δz of 1 μm covering the entire thickness of the biofilm. Single image stacks contained between 45 and 50 cross sections. Channel scanning locations were at least 20 mm away from the inlet

and 6 mm from the outlet to compensate for fluid entrance and exiting effects on biofilm development.

Image analysis

Microscope images were processed in TIF format with the MATLAB toolbox PHLIP (http://www.itqb.unl.pt:1141/ ~ webpages/phlip/). Prior to analysis, the images were converted to a resolution of 636 × 636 pixels to accommodate the RAM of the computer running PHLIP. For image segmentation, the automated thresholding function of PHLIP was applied to each image stack. PHLIP allows automated batch processing of CLSM images and provides the user with the capability to extend image processing operations. Consequently, porosity was added as an additional structural feature function. The biofilm architecture parameters roughness, mean thickness, spatial spreading, surface area to volume ratio, biovolume and porosity were calculated after connected volume filtration to remove 'floating material' from the analysis. The morphology parameter mean thickness is defined as the average of the distribution of pixel heights in an image stack. Average mean thickness, as calculated for statistical analysis, indicates the average of all 21 mean thickness values obtained from the biofilm.

Statistical analysis

After image analysis, data for each of the six parameters were subjected to statistical analysis using the statistical software SAS v8.02. Significant differences between pairwise comparisons were determined by Tukey's test ($P < 0.05$). Eq. (1) represents the one-way repeated measure ANOVA design that compared, among experimental rounds, channels that experienced the first staining event on the same day to determine which architecture features were reproducible between flow cells. The variable y_{ij} represents the observed architectural parameter for the ith scan location and jth flow cell, μ is the overall mean value of the experiment, ρ_i corresponds to the effect of scanning location, τ_j corresponds to the effect of flow cell, and ε_{ij} is the experimental error. The same model was used to determine if biofilms were reproducible between channels for the same flow cell. In this case, y_{ij} represents the observed architectural parameter of the ith scan location and jth flow channel and τ_j represents the effect of flow channel.

$$y_{ij} = \mu + \rho_i + \tau_j + \varepsilon_{ij} \quad (1)$$

Two methods of ANOVA were utilized to determine if repetitive staining of Syto9 had an effect on biofilm architecture after a channel was stained 1, 2 and/or 3 times (day 5 of the experiment). The first method (ANOVA-1) analyzed each flow cell individually while the second method (ANOVA-2) treated flow cells as replicates. The ANOVA-1 method treated the 21 scanning locations as replicates using the repeated measures design shown in Eq. (1). The variables are as described above except y_{ij} represents the observed architectural parameter for the ith scan location and jth staining treatment and τ_j corresponds to the effect of staining treatment. The second method, ANOVA-2, treated each flow cell as replicates and compared the average value of the 21 scan locations for each channel using the randomized block design shown in Eq. (2). The variables are the same as described for ANOVA-1, except $\bar{y}_{ij}$ represents the observed architectural parameter for a channel averaged over 21 locations for the ith flow cell and jth staining treatment and ρ_i corresponds to the effect of a flow cell as a block.

$$\bar{y}_{ij} = \mu + \rho_i + \tau_j + \varepsilon_{ij} \quad (2)$$

Results and discussion

The first objective was to identify biofilm measures that could be used to describe reproducible features of biofilm architecture. Statistical analysis compared the channels that experienced their first staining event on the same day to determine if biofilm architecture was reproducible among flow cells. Of the six characteristics calculated by PHLIP, the parameters: roughness, porosity, spatial spreading, and surface area to volume ratio showed significant differences. In contrast, the parameters: mean thickness and biovolume did not vary (Table 1). Consequently, these two characteristics were utilized to investigate the second objective concerning the effect of repetitive Syto9 staining on biofilm architecture. Significant differences were observed among staining treatments for biovolume and mean thickness when analyzed with ANOVA-1, which considers flow cells individually and each scan location as a replicate.

The average biovolume was significantly altered in those channels that had previously been exposed to Syto9 in 2 of 3 experiments on day 5 (Table 2). This trend is also apparent when biovolume is analyzed as a function of channel location (Figure 1). In experiment 2, the average biovolume in channel 3 (stained only once) was higher at $8.68 \times 10^4\,\mu m^3 \pm 0.35 \times 10^4\,\mu m^3$ ($\pm$ SEM) than in channels 1 and 2 at $6.33 \pm 0.21 \times 10^4\,\mu m^3$ and $5.19 \pm 0.27 \times 10^4\,\mu m^3$, respectively (Table 2, Figure 1A). In experiment 3 the average biovolume in channel 3 ($6.72 \pm 0.26 \times 10^4\,\mu m^3$) was less than the average biovolume in channel 2 ($9.49 \pm 0.36 \times 10^4\,\mu m^3$), which had been stained twice. However, the average biovolume of channels 2 and 3 was greater than that of channel 1 ($4.28 \pm 0.46 \times 10^4\,\mu m^3$), which had been stained three times (Table 2, Figure 1B).

Similar to the biovolume results, average mean biofilm thickness was significantly reduced in 1 of 3 experiments on day 5 for those channels that had previously been exposed to Syto9 (Table 2). The average biofilm thickness in experiment 3 for channel 3

Table 1 Reproducibility of biofilm architecture characteristics from three independent flow cells†

	Statistically significant differences among experiments‡		
Feature	**Day 3**	**Day 4**	**Day 5**
Biovolume	No	No	No
Mean thickness	No	No	No
Roughness	Yes	Yes	Yes
Porosity	No	No	Yes
Total spreading	No	Yes	Yes
SA to BV	Yes	No	Yes

†Only biofilms experiencing the first staining event were compared
‡repeated measures one-way ANOVA with $P < 0.05$

Table 2 Effect of repeated staining with Syto9 on biofilm architecture

		Day 5 ($\pm$SEM)		
Feature	**Staining**	**Exp 1**	**Exp 2**	**Exp 3**
Biovolume ($\times 10^4\,\mu m^3$)	1 ×	7.08 ± 1.49	8.68 ± 0.35†	6.72 ± 0.26‡
	2 ×	8.90 ± 1.22	5.19 ± 0.27†	9.49 ± 0.36‡
	3 ×	8.00 ± 1.24	6.33 ± 0.21†	4.28 ± 0.46‡
Mean thickness (μm)	1 ×	18.5 ± 1.3	21.8 ± 0.5	24.2 ± 0.6*
	2 ×	20.2 ± 1.2	20.9 ± 0.5	23.0 ± 0.7*
	3 ×	20.1 ± 1.3	21.5 ± 0.6	20.7 ± 0.5*

†, ‡, *Significant differences found between values for indicated feature and experiment using ANOVA-1 with $P < 0.05$

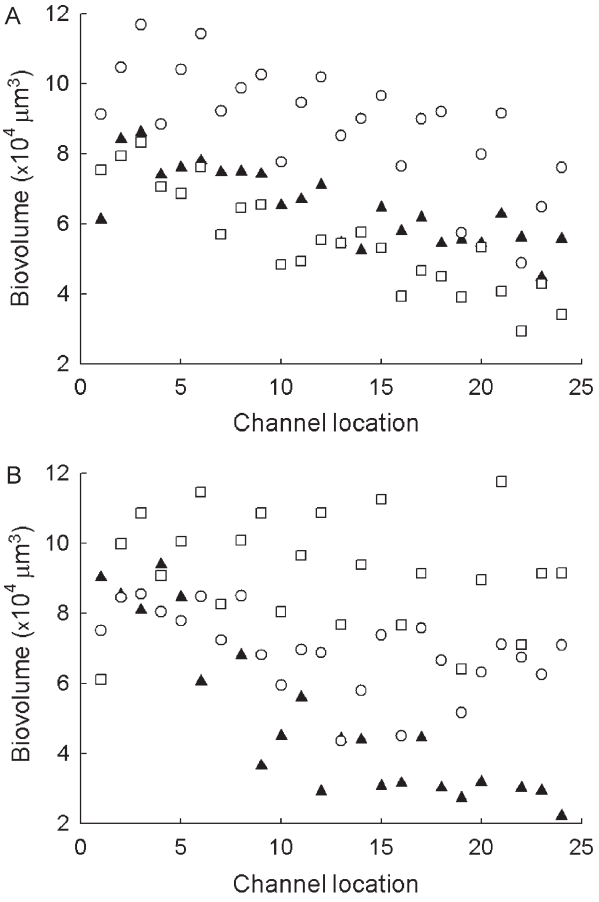

Figure 1 Plot of biofilm biovolume versus channel location for day 5 of Experiment 2 (A) and 3 (B). ▲, Channel 1; □, Channel 2; ○, Channel 3. Channel 1 was stained with Syto9 on days 3, 4, and 5; Channel 2 was stained on days 4 and 5; and Channel 3 was stained only on day 5. See text for discussion

(stained only once) was higher at 24.2 μm ± 0.6 μm (± SEM) than in channels 1 and 2 at 20.7 ± 0.5 μm and 23.0 ± 0.7 μm, respectively. In particular, channel 1, stained three times, had the thinnest biofilm based on average mean thickness.

Biovolume and mean thickness did not differ significantly among channels that experienced a single staining event on the same day (Table 1). Hence, we conclude that repeated staining with Syto9 resulted in a decrease in biovolume and mean thickness. In contrast, ANOVA-2, which treats each flow cell as a replicate and compares the average of the 21 scan locations, did not find significant differences among the staining treatments for any of the six structural features suggesting Syto9 did not have an effect on biofilm architecture. The contradictory results of ANOVA-1 and ANOVA-2 prompted an analysis to verify that biofilm architecture was reproducible between channels of the same flow cell.

One-way repeated measure ANOVA performed on identically treated channels within the same flow cell found significant differences among each of the six architecture parameters indicating biofilm structure was not reproducible between channels. This result suggests that the significant differences found with ANOVA-1 (Table 2) are not statistically discernable from inherent structural variation. However, the variability among channels of the same flow cell was considerably less than the variability among channels of

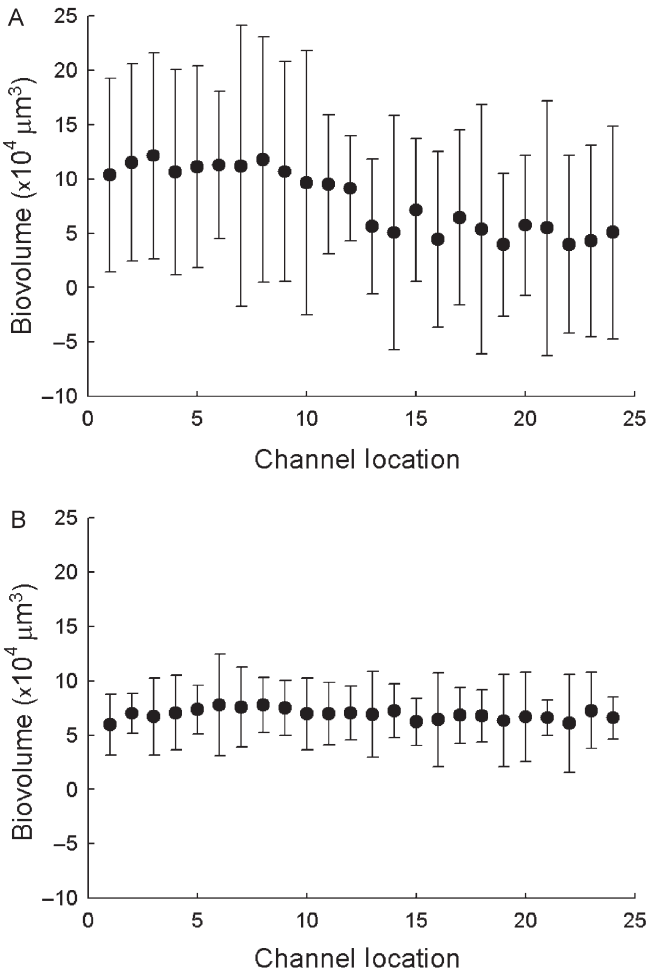

Figure 2 Comparison of biovolume variability on day 5 of development between flow cells (A) and between channels within the same flow cell (B). Error bars represent a 95% confidence interval with N = 3 (A) or N = 4 (B). Figure 2(A) contains locations 1–3 not considered in statistical analysis due to channel outlet proximity

different flow cells as illustrated for biovolume (Figure 2). This result suggests that the effects of Syto9 on architecture were not measurable above the high variability observed between flow cells and thus not identified by ANOVA-2. Although these results seem to question the role of Syto9, its effects became apparent for each of the three experimental rounds after visual inspection of biofilm images (not shown). It is by considering visual interpretation that the results of ANOVA-1 in Table 2 cannot be disregarded, and we conclude that unstained biofilms developed into thicker structures and contained more biomass.

Previous work has shown that reproducibility can be obtained in flow cell channels in the absence of repetitive staining for very young biofilms (Venugopalan *et al.*, 2005) or utilizing fluorescent proteins to track cells (Heydorn *et al.*, 2000a, b), at least until the first sloughing event (Lewandowski *et al.*, 2004). However, these studies obtained images with a 40× objective. When looking at a defined area, the heterogeneity of a biofilm is expected to be less pronounced at a magnification of 40× compared to 63×, which is required for cellular resolution and identification of single cell events as previously

shown (Hendrickx *et al.*, 2003). The extent of variability of biofilm architecture is scale dependent. Thus observations made with increased magnification can adversely affect both the reproducibility of biofilm structure and the ability to distinguish treatment effects from inherent differences. For instance, Beyenal *et al.* (2004) found the standard deviation to be greater at 100 × magnification than at 40 × magnification for the architectural parameters of areal porosity, fractal dimension, energy, and homogeneity when comparing 20 images of the same biofilm.

This study exemplifies the necessity of conducting flow channel experimentation with multiple replicate flow cells to obtain statistically significant results. In the case of biovolume the required number of flow cells to detect a difference greater than that observed from inherent variation, while maintaining a power of 90% and a significance level of 95% for three treatment effects, is greater than 27. This staggering number, calculated using Table B.12 from Neter *et al.* (1996), is primarily a consequence of the high standard deviation of replicate flow cell experiments and emphasizes the need to maintain stringent controls on experimental and environmental factors. One such factor is temperature, which has been reported to significantly affect biofilm architecture (Heydorn *et al.*, 2000a). If the standard deviation between flow cells was maintained at a level comparable to flow channel reproducibility then 8–10 flow cells would be required to detect a statistically significant effect of Syto9 treatment.

Conclusions

Acinetobacter sp. BD413 producing relatively homogeneous biofilms was employed to test the validity of using repeated nucleic acid staining to monitor biofilm development online by CLSM. Such an approach would greatly simplify the application of *in situ* investigations of nascent natural biofilms grown in reactors. Measurements were taken after an apparent steady-state was reached, and a number of structural parameters were determined.

The study identified the difficulties associated with achieving reproducible biofilm growth in parallel flow cells when high magnification is used to study biofilm architecture.

Two ANOVA-based statistical approaches analyzing either each flow cell separately (ANOVA-1) or as replicates (ANOVA-2) led to different conclusions regarding the effect of the nucleic acid stain Syto9 on biofilm development. Despite the difficulty of distinguishing repetitive Syto9 staining effects from inherent biofilm architecture variability, manual image inspection supports the results of ANOVA-1 (Table 2). Consequently, the use of Syto9 to visualize cells during biofilm development is not recommended as it affected both biovolume and mean thickness in treated flow channels.

Conceivably, the effect of Syto9 staining would be even more pronounced if applied at an earlier stage during biofilm development before the establishment of an apparent steady state as determined by biofilm thickness.

The results do not provide an unequivocal explanation for the biological effects of Syto9 and it is not known if the decrease in biomass is due to reduced growth rates or an increase in detachment.

We suggest that experimental biofilm architectures must be defined in rigorous mathematical terms and coupled with visual inspection when microscopic studies investigating phenomena at the cellular level are conducted.

Acknowledgements

R. GrayMerod acknowledges partial support by an industry supported fellowship under the Training Program in Biomolecular Technology at the University of California, Davis and from the NEAT-IGERT program sponsored by the National Science Foundation

(IGERT Grant DGE-9972741). J.B. Xavier was funded by the F.C.T./M.C.T.E.S., Portugal, grant SFRH/ BPD/ 11485/ 2002. The authors thank Dr. Shrini Upadhyaya and Dr. Neil Willits for their advice on ANOVA design.

References

Beyenal, H., Lewandowski, Z. and Harkin, G. (2004). Quantifying biofilm structure: Facts and fiction. *Biofouling*, **20**, 1–23.

Cowan, S.E., Gilbert, E., Khlebnikov, A. and Keasling, J.D. (2000). Dual labeling with green fluorescent proteins for confocal microscopy. *Appl. Environ. Microbiol.*, **66**, 413–418.

Hendrickx, L., Hausner, M. and Wuertz, S. (2003). Natural genetic transformation in monoculture *Acinetobacter* sp. strain BD413 biofilms. *Appl. Environ. Microbiol.*, **69**, 1721–1727.

Heydorn, A., Ersboll, B.K., Hentzer, M., Parsek, M.R., Givskov, M. and Molin, S. (2000a). Experimental reproducibility in flow-chamber biofilms. *Microbiology-UK*, **146**, 2409–2415.

Heydorn, A., Nielsen, A.T., Hentzer, M., Sternberg, C., Givskov, M., Ersboll, B.K. and Molin, S. (2000b). Quantification of biofilm structures by the novel computer program COMSTAT. *Microbiology-UK*, **146**, 2395–2407.

Kuehn, M., Hausner, M., Bungartz, H.J., Wagner, M., Wilderer, P.A. and Wuertz, S. (1998). Automated confocal laser scanning microscopy and semiautomated image processing for analysis of biofilms. *Appl. Environ. Microbiol.*, **64**, 4115–4127.

Kuehn, M., Mehl, M., Hausner, M., Bungartz, H.J. and Wuertz, S. (2001). Time-resolved study of biofilm architecture and transport processes using experimental and simulation techniques: the role of EPS. *Wat. Sci. Tech.*, **43**(6), 143–150.

Lewandowski, Z., Beyenal, H. and Stookey, D. (2004). Reproducibility of biofilm processes and the meaning of steady state in biofilm reactors. *Wat. Sci. Tech.*, **49**(11–12), 359–364.

Neter, J., Kutner, M.H., Nachtsheim, C.J. and Wasserman, W. (1996). *Applied Linear Statistical Models*, Fourth edition, McGraw-Hill, Inc., New York.

Venugopalan, V.P., Kuehn, M., Hausner, M., Springael, D., Wilderer, P.A. and Wuertz, S. (2005) Architecture of a nascent *Sphingomonas* sp. biofilm under varying hydrodynamic conditions. *Appl. Environ. Microbiol.*, **71**, 2677–2686.

Xavier, J.B., Picioreanu, C. and van Loosdrecht, M.C.M. (2004). Assessment of three-dimensional biofilm models through direct comparison with confocal microscopy imaging. *Wat. Sci. Tech.*, **49**(11–12), 177–185.

Xavier, J.B., Schnell, A., Wuertz, S., Palmer, R., White, D.C. and Almeida, J.S. (2001). Objective threshold selection procedure (OTS) for segmentation of scanning laser confocal microscope images. *J. Microbiol. Meth.*, **47**, 169–180.

Yang, X.M., Beyenal, H., Harkin, G. and Lewandowski, Z. (2000). Quantifying biofilm structure using image analysis. *J. Microbiol. Meth.*, **39**, 109–119.